

**Modeling T1 Resting-State MRI Variants Using Convolutional Neural Networks in
Diagnosis of OCD**

Tarun Eswar

Massachusetts Academy of Math & Science

Advanced STEM with Scientific and Technical Writing

Instructors: Mr. Nicholas Medeiros, Kevin Crowthers, Ph.D.

Worcester, MA. 01605

Acknowledgements

I would like to give a special thanks to Dr. Kevin Crowthers and Mr. Nicholas Medeiros for their support throughout the journey of this research project. Additionally, I am grateful for the help provided by Varshini Ramanathan of Tufts University as well as Revathi Ravi of Massachusetts General Hospital for their guidance in topic-specific knowledge as well as with data needs. Finally, I am thankful for the guidance provided by Joseph Yu in aiding my understanding of machine learning concepts for this project.

Abstract

Obsessive-compulsive disorder (OCD) presents itself as a highly debilitating disorder. The disorder has common associations to the prefrontal cortex and the glutamate receptor known Metabotropic Glutamate Receptor 5 (mGluR5). This receptor has been observed to demonstrate higher levels of signaling from positron emission tomography scans measured by its distribution volume ratios. Though, studies are unable to verify the involvement of mGluR5. Computational modeling methods were used as a means of validation for previous hypotheses involving mGluR5. The inadequacies in relation to the causal factor of OCD were answered by utilizing T1 resting-state magnetic resonance imaging (TRS-MRI) scans of patients suffering from schizophrenia, major depressive disorder, and obsessive-compulsive disorder. Because comorbid cases often occur within these disorders, cross comparative abilities become necessary to find distinctive characteristics. After unique structures of tissues found in OCD TRS-MRI scans were identified, a gene expression analysis was conducted based on scan data output. Two-dimensional convolutional neural networks alongside ResNet50 and MobileNet models were constructed and evaluated for efficiency. Activation heatmaps of TRS-MRI scans were outputted, allowing for transcriptomics analysis. Though, a lack of ability of prediction of OCD cases prevented gene expression analysis. Across all models, there was an 88.75% validation accuracy for MDD, and 82.08% validation accuracy for SZD under the framework of ResNet50 as well as novel computation. OCD yielded an accuracy rate of ~54.4%. These results provided further evidence for the *p* factor theorem regarding mental disorders. Future work involves the application of transfer learning to bolster accuracy rates.

Keywords: Obsessive-compulsive disorder, magnetic resonance imaging, major depressive disorder, schizophrenia

Modeling T1 Resting-State MRI Variants Using Convolutional Neural Networks in Diagnosis of OCD

Over recent decades, obsessive compulsive disorder (OCD) has been ranked as one of the ten most disabling disorders (Murray and Lopez, 1996). A patient suffering from OCD will often experience a variety of symptoms that fall into two main categories: obsessions and compulsions. Obsessions refer to being overly focused on a specific issue, involving overthinking in the form of impulsions. Furthermore, compulsions reflect specific actions in order to counteract the obsessive symptoms. These habits can include checking and mental compulsions, though the list of specific compulsions varies by case (International OCD Foundation, 2010). The symptoms themselves seem relatively benign; however, concern arises in relation to how much time the disorder occupies in a sufferer's daily life. The fear associated with failing to fulfill an impulse is the major component in the factors that push a diagnosed patient to follow their obsession(s). As a result, a sufferer of OCD typically spends an hour or more each day fixated on these debilitating symptoms (NIMH, 2019). Those facing extreme cases of OCD can often endure increased disruptions to daily life, including the inability to participate at places of work or in school (Wood, 2018).

Though OCD has been established as a severely debilitating condition, treatments and knowledge of the disorder are still developing. Current treatments involve utilizing Selective Serotonin Reuptake Inhibitors (SSRIs) as prior research hypothesized serotonin to be a target for effective treatment to the disorder. However, when tested, 40 to 60 percent of patients noticed zero to partial improvements to their symptoms (Kellner, 2010). Low success rates with this specific class of drug demonstrate a lack of understanding in the realm of targeting the source of OCD; however, the issue is further convoluted by SSRIs remaining the most common choice for

medicating OCD patients (Xu et al., 2021). Rather than focusing on serotonin-based solutions, glutamate-based treatments have risen as a novel approach in regard to understanding the causal factors involved. Nevertheless, findings based on glutamate could be difficult to generalize as the substance is abundant in the brain and underpins various aspects of learning and memory; therefore, unintended consequences could abound as it is not clear that the substance could be targeted specifically for OCD with the exclusion of its other functions.

Glutamate is an excitatory neurotransmitter, with the function of stimulating nerve cells that send a chemical message between differing nerve cells. Glutamate itself is made from glial cells in the brain and is recycled as the older glutamate is simply refreshed with new glutamate naturally. Beyond serving the different trigger actions, glutamate also helps to process gamma-aminobutyric acid, which is another neurotransmitter to calm the brain. In the body, glutamate serves to enhance learning and memory, energy sources for brain cells, chemical messengers, sleep-wake cycles, and pain signaling. Therefore, in the scope of OCD where obsessive behaviors—such as constant checking—are prevalent, the involvement of glutamate becomes a potential. Furthering this notion is the past research conducted with glutamate. At Ruhr University in Germany, researchers were able to determine that excessive glutamate led to a higher cerebrospinal fluid level in OCD patients compared to non-OCD patients. High levels of glutamate were also observed in OCD patients based on a magnetic resonance spectroscopy scan at Wayne State University (International OCD Foundation, 2010). In order to confirm correlation, gene expression data in varying regions of the brain can confirm up-regulation of GRM, validating involvement of glutamate.

However, with the case of GRM, the only method to test the levels of specific receptor values is through distribution volume ratios that utilize positron emission tomography (PET)

scans. At first, this method presents a viable solution to the issue; however, another systematic adequacy occurs in that PET scan data is difficult to find for obsessive-compulsive disorder. Rather, T1 resting-state MRI scans can be substituted for analysis. These scans can identify structural regions of the brain, unnoticeable to the human eye, that deviate across disorders. Gene expression analysis based on these scans then provides an outlet to map MRI scans to data points that undergo analysis.

Problem Statement

Determining the root cause of obsessive-compulsive disorder is highly difficult. Physicians are often unable to differentiate obsessive-compulsive disorder from major depressive disorder and schizophrenia. As a result, the overall aim of this project was to design models for each disorder, develop activation heatmaps, and extract regions of interest. These models serve as a steppingstone in reaching significance of GRM in OCD patients. In order to supplement these models, gene expression analysis was conducted afterwards in order to determine the involvement of mGluR5, encoded by GRM, in OCD patients.

Engineering Objective

Diagnosis of OCD is currently understudied and misunderstood within the field of neuroscience. On basis of these observations, a few main objectives were enacted:

Obj. 1a: Construct individual CNNs with guidance from pre-trained networks for OCD, MDD, and Schizophrenia respectively with accuracy rates of at least 80%.

Obj. 1b: Develop activation heatmaps, demonstrating regions of interest unique to each disorder.

Obj. 1c: Perform gene expression analysis on T1 resting-state MRIs with transcriptomics.

Obj. 1d: Provide an online web application to allow patients to receive data from the models details in Obj. 1a, as well as to feed more data into the models.

Research on obsessive-compulsive disorder in regard to root causes is still misunderstood because of privatization of datasets and knowledge. As a result, Obj. 1d provides a method to aid future research in being able to expand upon past knowledge in a more accessible and reasonable manner. Obj. 1d will also allow for patients to receive helpful metrics free of charge.

Section II: Methodology

Role of Student vs. Mentor

Over the span of 6 months, I conducted work within the general area of machine learning. With respect to this project, I take accountability for the work done with modeling and results. I received guidance from my advisors in developing my ideas as well as how to probe further into findings. I also received assistance in developing a mastery of machine learning-based technologies from my mentors.

Equipment and Materials

In order to achieve the objects outlined, a plethora of resources were utilized. Models were constructed on Python 3.10.0 with TensorFlow Keras. Within these models, numerous technologies were required for development: SimpleTK, Pandas, Matplotlib, NumPy, MedPy, Skimage, seaborn, ResNet50, MobileNet, Scikit-learn, NPM, node.js, AWS and Imaging-transcriptomics.

Furthermore, in terms of hardware, this project was conducted using a 2022 Apple MacBook Pro (M2 processor, 8GB ram). Additionally, parts of the models were constructed on a 2022 Apple MacBook Mini (M2 processor, 8GB ram).

Datasets

In order to construct models for the disorders in question, T1 resting-state MRI is required in plentiful amounts for each. Data acquired for MDD was sourced from Bezmaternykh D.D et al. 2021. This database contains 72 patients with T1 resting-state MRI scans. Repetition time for these scans was 2.5 seconds with a 90-degree flip angle. T1 resting-state MRI scans for schizophrenia were acquired from Poldrack, R. et al. 2021. The dataset from Poldrack, R. et al.

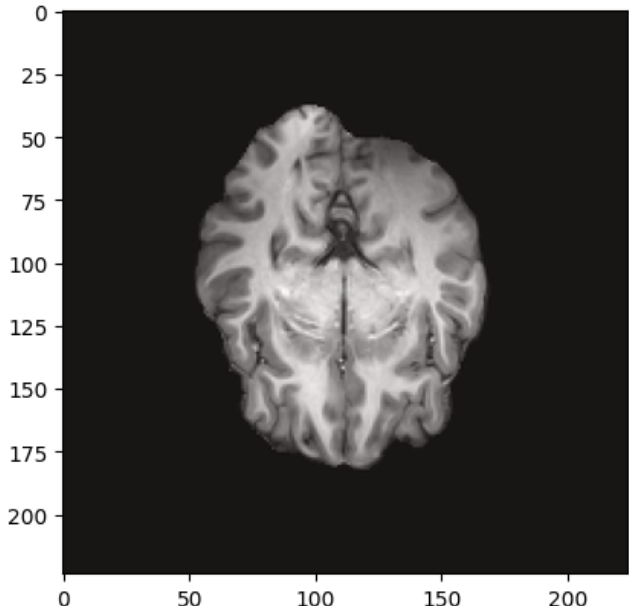


Figure 1. TRS-MRI Sample

An example of a 2D resting-state MRI scan acquired from the UCLA Consortium and pre-processed with NumPy.

provided MRI scans for several disorders, though only schizophrenia and control patients were used. OCD T1 fractional anisotropy scans were sourced from Kim, Seung-Goo et al., 2015. Each of these datasets were pre-processed with NumPy resizing techniques to fit the data to size requirements. Afterwards, scikit-learn distributed the datasets into the configuration of 70% train, 30% test (Nguyen, 2021). Missing anatomy subfolders were excluded prior to model creation. Incorrectly sized images or mistimed scans were also subject to removal. AWS and npm were utilized for large file downloads from the databases.

Novel 2D CNNs

Novel 2D convolutional neural networks were established for each disorder to provide proof of concept for further testing. Each novel CNN was composed of a sequential base, containing pooling, batch, and dropout layers to condense T1 MRI slices into a 1x1 matrix

within the sigmoid layer. The model compiled with an Adam optimizer to reduce computation time (Yi, D., Ahn, J., & Ji, S., 2020). Furthermore, this optimization allowed for an easier load during the course of this proof of concept. Each model compiled over 25 epochs with a batch size of 32, amounting to roughly 11.7 hours of runtime per each trial.

Optimized Neural Networks

Pre-trained frameworks were used post confirmation of functioning novel models. Slices were re-scaled by a scale factor of 0.874 per ResNet50 requirements. During pre-processing, slices with differentiating time stamps due to issues within the scan were excluded. Furthermore, T1 MRI scans noted as corrupted or missing by the primary author of each dataset were also excluded. During the usage of ResNet50, the ram requirement for 23.2 billion parameters surpassed the number of resources available with the given hardware. As a result, the central 40 scans per each disorder model were utilized to allow for model compilation. As per ResNet requirements, the coordinate arrays from STIK were stacked by 3 and fitted to the respective shape per disorder (X, Y, 3). The default weight of ImageNet from ResNet50 was in use for modeling. The model ran with a base learning rate of 0.001 throughout the course of 30 epochs. The first 10 epochs were run without interference from ResNet weights whereas pre-trained models and the activation of ImageNet executed from epoch 10 onwards. A similar approach was adapted in order to make use of MobileNet.

Activation Heatmaps

Activation heatmaps of the neural network models were created following model development. In order to construct heatmaps, testing data was classified based on the prediction attribute of the model. Afterwards, the layer at index -1 was extracted to obtain weights of size 2048. Based on the usage of ResNet, the final conv layer, conv5_block3_out, was extracted at

size 7, 7, 1. This matrix was then resized to T1 resting-state size of 189 X 189 X 2048 in order to provide an overlay of the heatmap onto the original MRI. Cmap of “jet” was incorporated at an alpha level of 0.5 to highlight regions of importance per each disorder.

Statistical Tests

In order to analyze the performance of the models, the F1 score, and confusion matrix were generated. Additionally, the Matthews Correlation Coefficient score was analyzed. These metrics were selected based on their specificity to machine learning models (Goutte, C., & Gassier, E., 2005). Classifying the results of a model by means of the traditional statistics were averted on basis of variation in datasets and methodology.

Section III: Results

Dataset Creation

In the initial stages of this project, large datasets from a variety of sources were compiled prior to analysis. In total, over 150 sub-sessions of T1 resting-state scans were developed through the course of this project. In light of limited data accessibility, acquiring data of this amount presents as a means for an ease in future use of finding MRI-related datasets.

Novel 2D CNNs

Through the course of model development, the novel 2D CNN was utilized as a means of providing reliable evidence of functionality prior to moving forward. In the case of MDD, the model accuracy approached 99.34% as the validation accuracy flattened at 73.44%. Figure 1 demonstrates the variance in accuracy of the model over the span of 10 epochs. Furthermore, the statistical analysis technique of a confusion matrix was utilized for the novel models as shown in Figure 2. This measure allows the generalization of overall effectiveness of the model at a glance. Precision, recall, F1 and detailed analysis were constructed for definite pre-trained

models. These results enabled the usage of pre-trained neural networks. Furthermore, the novel 2D CNN constructed for schizophrenia also yielded promising results with a model accuracy of 99.77% and validation accuracy of 82.08%. Figure 3 depicts the rate of accuracy with respect to the epoch interval. Figure 4 demonstrates the confusion matrix for schizophrenia. Based on results provided from ResNet50, a novel model was not constructed for OCD.

Figure 1. MDD Validation

Validation and model accuracy metrics over the interval of 10 epochs for MDD.

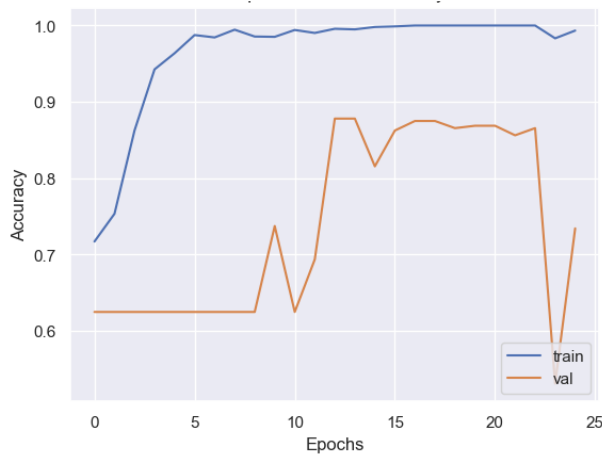


Figure 2. MDD Confusion Matrix

Confusion matrix statistical analysis for MDD model performance and accuracy.

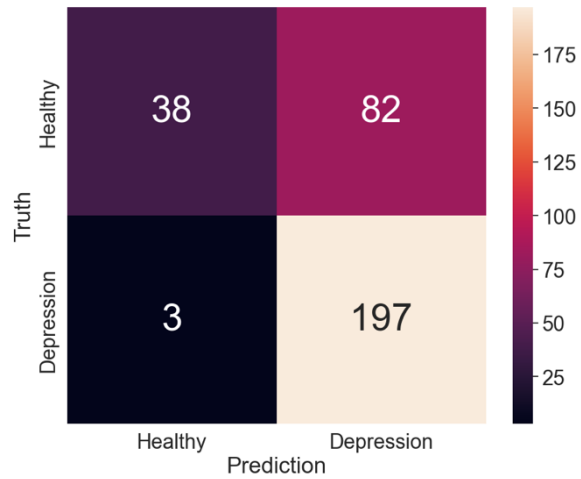


Figure 3. SZD Validation

Validation and model accuracy metrics over the interval of 10 epochs for schizophrenia.

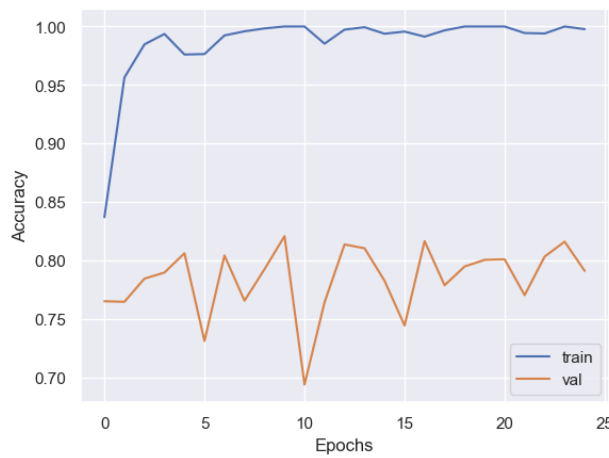
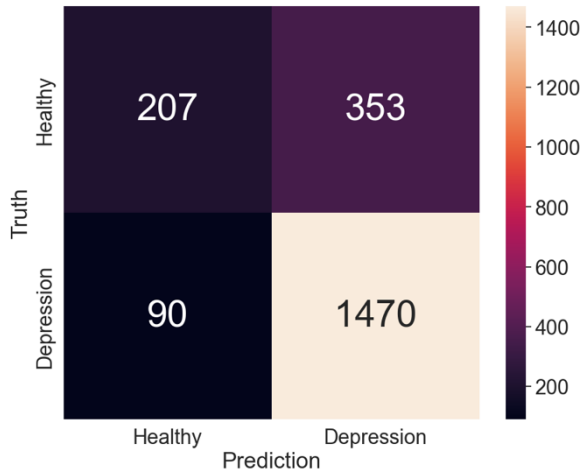


Figure 4. SZD Confusion Matrix

Confusion matrix statistical analysis for schizophrenia model performance and accuracy.



Optimized Neural Networks

After creation of novel networks, ResNet50 and MobileNet were investigated in order to achieve higher rates of validation accuracy. In order to visualize the variance created by the usage of a pre-trained network, a green fine-tuning line is incorporated at epoch 10. For MDD, validation approached the limit of 1.00 while the validation accuracy stabilized at 88.75%. Cross entropy readings fluctuated but reached natural deviation after epoch 15.

Table 1.

Statistical Measures Based on RESNET_depression_resting_state_dataset_t1_2d.h5

Precision	0.6000
F1 Score	0.7423
Matthews Correlation Coefficient	0.6774
Sensitivity	0.9730
Specificity	0.8049

Figure 5. ResNet50 MDD Validation

ResNet50 validation and cross entropy with respect to change in epoch.

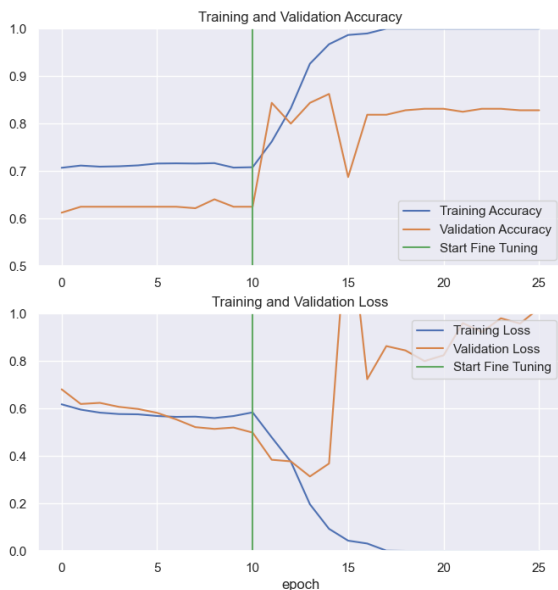


Figure 6. ResNet50 MDD Confusion Matrix

ResNet50 confusion matrix based on model performance.

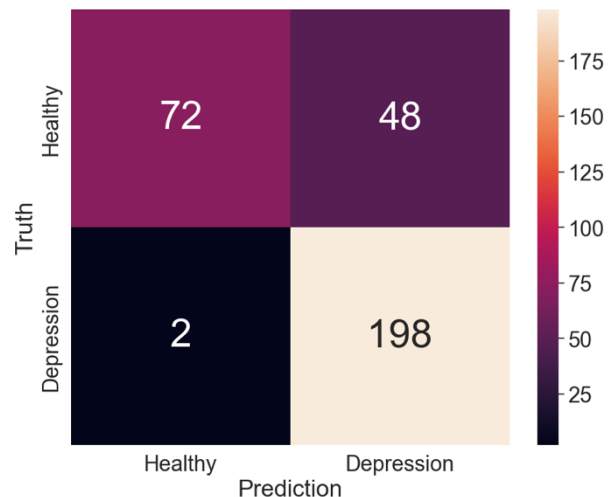


Figure 5 demonstrates the change in accuracy and cross entropy over time while Figure 6 is the corresponding matrix results. Similar results were produced in regard to the Schizophrenia ResNet50 model. Patient 126 was excluded from the sample due to image framing difficulties. Afterwards, the remaining scans were cross validated for shape as shown in Figure 10. The model yielded a validation accuracy of 80.5% and a model accuracy that approached the 99.9%. Prior to fine tuning, the model averages validation accuracy in ~70% range. After weight and pre-train activation, the model climbs in terms of model accuracy, though the validation accuracy remains stable as shown in Figure 8. Resulting statical measures are shown in Table 2.

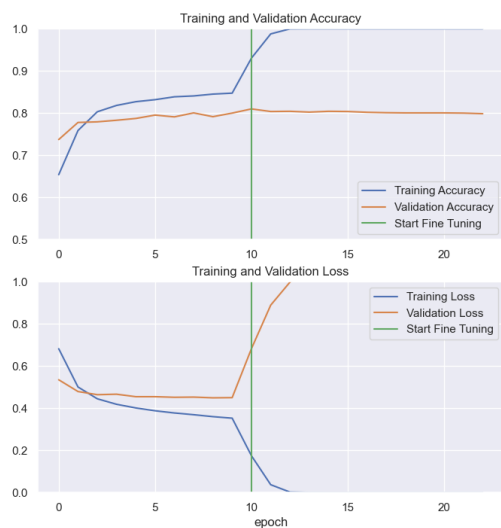
Table 2.

Statistical Measures Based on RESNET_schizophrenia_resting_state_dataset_t1_2d.h5

Precision	0.5786
F1 Score	0.6166
Matthews Correlation Coefficient	0.4928
Sensitivity	0.6599
Specificity	0.8551

Figure 8. ResNet50 SZD Validation

ResNet50 validation and cross entropy with respect to change in epoch for schizophrenia.

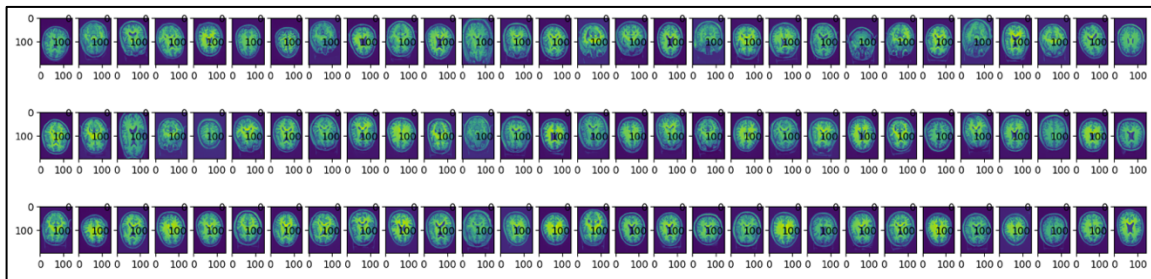
**Figure 9. ResNet50 SZD Confusion Matrix**

Confusion matrix generation for performance of the ResNet50 schizophrenia model.



Figure 10. Verifying SZN TRS-MRI Data

Remaining T1 resting-state MRI scans after removal of sub-126. Shape validation was conducted on these scans for dimensions (151, 40, 199).



When conducting model for OCD, both the model and validation accuracies yielded levels around ~54.44%. Furthermore, the confusion matrix resulted in 0 predicted slices of OCD while the remaining 120 were classified as healthy by the model.

Figure 11. ResNet50 validation and cross entropy with respect to change in epoch for OCD.

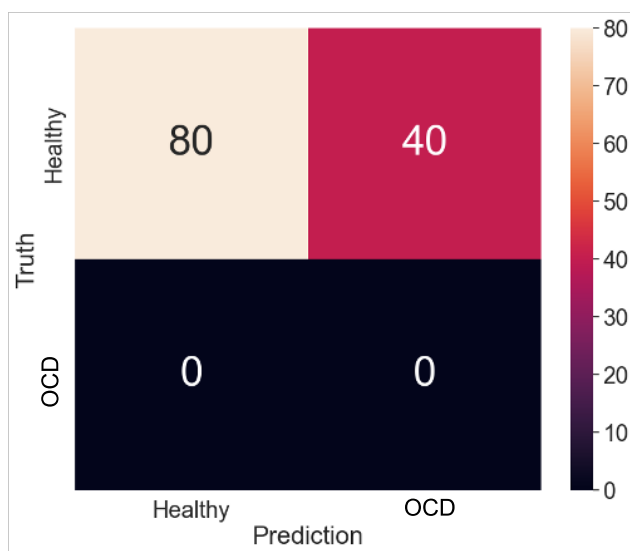
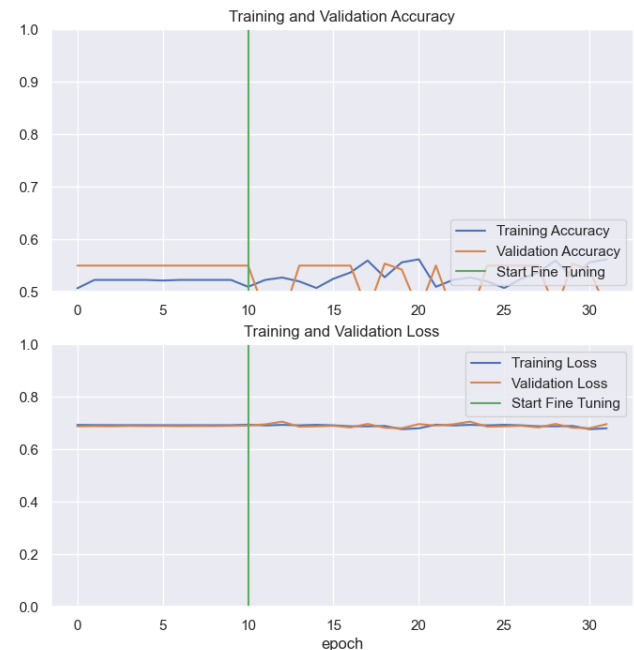


Figure 12. ResNet50 validation and cross entropy with respect to change in epoch for OCD.



Activation Heatmaps

After confirming relatively fair accuracy within the models constructed, activation heatmaps were constructed. Scaled convolution layers were placed over the original image in order to extract the regions of interest. Cmap “jet” outputted the heatmaps as zones. Red and orange zones are representative of areas in which the neural network detected differences in structural patterns. Heatmaps were not outputted for OCD. Figure 13 depicts the heatmap configuration for MDD while Figure 14 demonstrates the configuration for schizophrenia. Partial scans from schizophrenia are displayed; all heatmaps can be found in the appendix.

Figure 13. MDD Activation Heatmaps.

The figures below demonstrate the activation heatmaps cast onto the 72 patients within the MDD model.

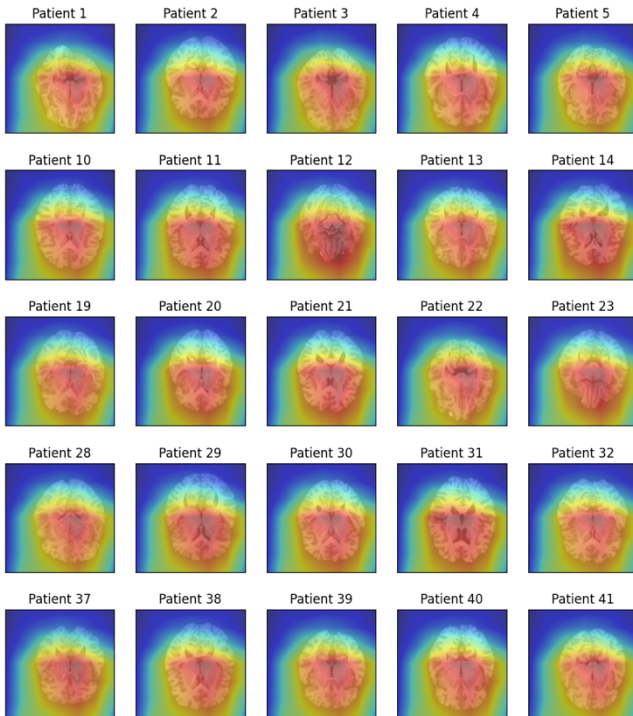
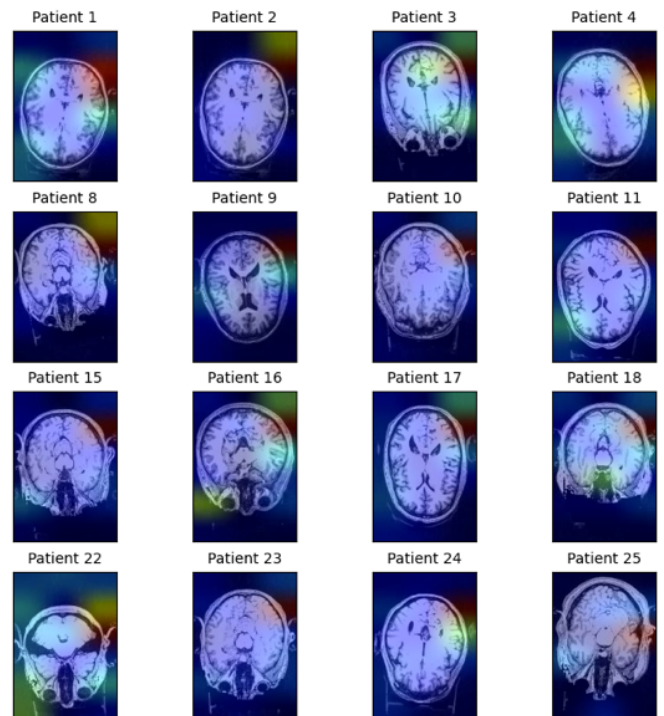


Figure 14. Schizophrenia Activation Heatmaps.

The figures below demonstrate the activation heatmaps for the schizophrenia model. Regions of red are areas of interest in diagnosis.



Section IV: Discussion

Prior to completing the study, the overarching goal for this project was to develop a respective classification model for OCD, SZD, and MDD. From these models, heatmaps became an additional objective in order to provide an overview of regions of interest for the 2D CNN. Furthermore, these models were intended to be used in gene expression analysis in order to identify significant gene encodings that demonstrate higher levels of influence in OCD as compared to other disorders. A final objective was a web application implementation was left as a final objective. A two-proportion z test was utilized throughout all model cases due to the nature of the data: varying percentages requiring a metric to be standardized and compared.

Through conducting this study, respective models for MDD, SZD, and OCD have been constructed. Though successful in construction, each demonstrates an important and different aspect in term of OCD. MDD provided a validation accuracy of 88.75%. Within the field of computational neuroscience, this accuracy serves to provide more reliable results as compared to other models. When compared to other models, our MDD classification network produced a P-Value of ~0.04363, significant at an alpha level of 0.05. Achieving this level of significance allows for the model to be presented as a viable classification method in the future. Additionally, the heatmap generation demonstrated implications in the corpus callosum. This finding is consistent with past literature (Lee, 2020). By demonstrating further support of the involvement of the corpus callosum, future research can have greater assurance in results on basis of our work.

Furthermore, schizophrenia provided similarly assuring results as with MDD. In order to test the concept of computational modeling, a novel network was built as a primary mean. Though we theorized that shifting to ResNet50 to bolster accuracy with ImageNet, the novel

network provided a greater level of accuracy at 82.08% in comparison to the optimized network. This novel network was not optimized per layer, meaning that future work has the potential to bolster accuracy rates for the novel network without the means of transfer learning. The GradCam heatmaps demonstrates implications within the right frontal lobe. Determining the importance of the right frontal lobe, or more broadly the frontal lobe, aligns with previous works within the field of neuroscience (Mubarik, 2016). These results have the ability to narrow down future research regarding schizophrenia.

Unlike MDD and SZD, the OCD novel and optimized networks failed to predict healthy from OCD patients. When first observing the results, this failure appeared to be the cause of TRS-MRI distortions during the scans from the dataset; however, further analysis demonstrated that the framework was able to sufficiently read the coordinate points of scans. Furthermore, the authors of the data with FSL (Kim, Seung-Goo et al., 2015). As a result, OCD is evidenced to possess no characteristics that define it from a healthy brain, leading to the inability of prediction. As demonstrated by the confusion matrix in Figure 11, the model outputted that all scan slices were healthy patients. If no defining characteristic can be found by the classification network, it must default to healthy as per the logistics of binary classification. These findings are consistent with a meta-analysis conducted by the ADAA. They found that across 100 studies collected, they were unable to find a consistency of OCD function implications that could be a cause of a cognitive aspect. In addition, they note that due to these inconsistency in findings across studies, pushing towards adequate treatments in the future becomes increasingly difficult (ADAA, 2022). Our model summarizes these descriptions by the author by demonstrating the idea that because of implications in multiple reasons, the model fails to provide a viable method

to predict future cases. Therefore, the objective for OCD TRS-MRI slices was not satisfied, but a deeper level of understanding of the field and its reflection within the model was understood.

Through the course of conducting this project, the major limitation faced was computing power. Due to the 8GB RAM limit, only certain subsets of data were able to be processed. Surpassing this barrier will allow for the usage of deep transfer learning in the form of a support vector machine in the future. Data acquisition arose as another limitation and restricted the project to publicly available datasets. For instance, this study intended to utilize PET scan data in the initial stages but switched to TRS-MRI due to data availability.

Though SZD and MDD neural networks point to specific regions of scan slices, the overall findings of this project further the “p factor theory.” This theory alludes to the fact that all psychopathological disorders can be generalized under one umbrella of disorders. Authors of this paper further contribute to the concept of being inability to utilize TRS-MRIs instating that groups attempting to neglect the “p factor” and find regions of interest tend to create contradictory results to preexisting studies (Marshall, 2020). Understanding disorders with lacking knowledge will require a utilization of the p factor. OCD lacks fundamental understanding; though, the use of the *p factor* presents a viable solution to treat OCD as well as other under-studied disorders in the future.

Future Research

Future research may involve the optimization of the models constructed in this paper. Though providing promising accuracy rates, model validation can be presented with deep learning methods. Furthermore, in terms of SZD and MDD, rather than being stratified into two separate disorders, future work may focus on condensing these models under one network that can differentiate the disorders across multiple classes. Creation of this combined model has the

potential to provide more supplementary evidence to the *p factor*. Providing further evidence for the *p factor* is essential to develop more effective and widely used treatments in the future.

Section V: Conclusion

Our engineering project served to identify the differentiation factor between OCD and disorders comorbid to OCD. As a result, SZD and MDD were selected for cross-comparative analysis. From there, the project served to generate heatmaps as well as a gene expression analysis model to determine the significance of gene encodings across the disorders. These objectives were set on basis that mGluR5 was implicated in those suffering from OCD. In order to conduct the study, this study focused on using convolutional neural networks to classify disorders, with the means of novel, ResNet50, and MobileNet models. Afterwards, heatmaps were generated in accordance with ResNet50 guidelines and with gradCam. However, prior to approaching the gene expression analysis stage, the TRS-MRI scans were unable to predict cases of OCD based on slices. As a result, on basis of prior studies, we interpreted that the model was unable to predict because of multiple regions facing implications in OCD. Though diverting from the original objective of finding the differentiation factor for OCD, the lack of prediction still points to a fundamental piece of motivation for this project—a lacking form of treatment for OCD. Lacking predictions, though, still provided a useful insight as they pointed towards a theory known as the *p factor*. This theory states that within the field of neuroscience, researchers are unable to find distinctive characters to respective disorders because disorders are not discrete. Rather, they fall onto a continuum of disorders that must be treated in an empirical manner rather than case-by-case. Though a singular factor was unable to be uncovered through this project, further support for the *p factor* was found. These findings guides future research and provides a feasible theory and mode to finding a treatment for OCD.

Section VI: References

- Abe, T., Sugihara, H., Nawa, H., Shigemoto, R., Mizuno, N., and Nakanishi, S. (1992). Molecular characterization of a novel metabotropic glutamate receptor mGluR5 coupled to inositol phosphate/Ca²⁺ signal transduction. *J. Biol. Chem.* 267, 13361–13368.
- Ade, K. K., Wan, Y., Hamann, H. C., O'Hare, J. K., Guo, W., Quian, A., Kumar, S., Bhagat, S., Rodriguez, R. M., Wetsel, W. C., Conn, P. J., Dzirasa, K., Huber, K. M., & Calakos, N. (2016). Increased Metabotropic Glutamate Receptor 5 Signaling Underlies Obsessive-Compulsive Disorder-like Behavioral and Striatal Circuit Abnormalities in Mice. *Biological psychiatry*, 80(7), 522–533.
<https://doi.org/10.1016/j.biopsych.2016.04.023>
- Akkus, F., Terbeck, S., Ametamey, S. M., Rufer, M., Treyer, V., Burger, C., Johayem, A., Mancilla, B. G., Sovago, J., Buck, A., & Hasler, G. (2014). Metabotropic glutamate receptor 5 binding in patients with obsessive-compulsive disorder. *The International Journal of Neuropsychopharmacology*, 17(12), 1915–1922.
<https://doi.org/10.1017/s1461145714000716>
- Bezmaternykh D.D., Melnikov M.Y., Savelov A.A. et al. Brain Networks Connectivity in Mild to Moderate Depression: Resting State fMRI Study with Implications to Nonpharmacological Treatment. *Neural Plasticity*, 2021. V. 2021. № 8846097. PP. 1-15. DOI: 10.1155/2021/8846097
- Funda Akkus, Sylvia Terbeck, Simon M. Ametamey, Michael Rufer, Valerie Treyer, Cyrill Burger, Anass Johayem, Baltazar Gomez Mancilla, Judit Sovago, Alfred Buck, Gregor Hasler. (2014). Metabotropic glutamate receptor 5 binding in patients with obsessive-compulsive disorder, *International Journal of Neuropsychopharmacology*, Volume 17, Issue 12, December 2014, Pages 1915–1922, <https://doi.org/10.1017/S1461145714000716>
- Goodman WK, Price LH, Rasmussen SA, et al. The Yale-Brown Obsessive Compulsive Scale: II. Validity. *Arch Gen Psychiatry*. 1989;46(11):1012–1016. doi: 10.1001/archpsyc.1989.01810110054008
- Goutte, C., & Gaussier, E. (2005). A Probabilistic Interpretation of Precision, Recall and F-Score, with Implication for Evaluation. In D. E. Losada & J. M. Fernández-Luna (Eds.), *Advances in Information Retrieval* (pp. 345–359). Springer. https://doi.org/10.1007/978-3-540-31865-1_25
- How to Go Deeper with Your OCD Research Data.* (2020). Retrieved February 9, 2023, from <https://adaa.org/learn-from-us/from-the-experts/blog-posts/professional/how-go-deeper-your-ocd-research-data>

International OCD Foundation. (2010). What is OCD? International OCD Foundation. <https://iocdf.org/about-OCD/>

International OCD Foundation. (2010). New Horizons in OCD Research and the Potential Importance of Glutamate.

Can We Develop Treatments That Work Better and Faster? (2010). International OCD Foundation.

<https://iocdf.org/expert-opinions/expert-opinion-glutamate/>

Kellner, M. (2010). Drug treatment of obsessive-compulsive disorder. *Dialogues in Clinical Neuroscience*, 12(2),

187–197. <https://www.ncbi.nlm.nih.gov/pmc/articles/PMC3181958/>

Lee, S., Pyun, S.-B., Choi, K. W., & Tae, W.-S. (2020). Shape and Volumetric Differences in the Corpus Callosum

between Patients with Major Depressive Disorder and Healthy Controls. *Psychiatry Investigation*, 17(9), 941–

950. <https://doi.org/10.30773/pi.2020.0157>

Marshall, M. (2020). The hidden links between mental disorders. *Nature*, 581(7806), 19–21.

<https://doi.org/10.1038/d41586-020-00922-8>

Mubarik, A., & Tohid, H. (2016). Frontal lobe alterations in schizophrenia: A review. *Trends in Psychiatry and*

Psychotherapy, 38, 198–206. <https://doi.org/10.1590/2237-6089-2015-0088>

McDougle, C. J., Goodman, W. K., Leckman, J. F., & Price, L. H. (1993). The psychopharmacology of obsessive

compulsive disorder. Implications for treatment and pathogenesis. *The Psychiatric clinics of North*

America, 16(4), 749–766.

Murray CJ Lopez AD (1996) The Global Burden of Disease. Boston, MA: Harvard University Press.

Nguyen, Q. H., Ly, H.-B., Ho, L. S., Al-Ansari, N., Le, H. V., Tran, V. Q., Prakash, I., & Pham, B. T. (2021).

Influence of Data Splitting on Performance of Machine Learning Models in Prediction of Shear Strength of

Soil. *Mathematical Problems in Engineering*, 2021, e4832864. <https://doi.org/10.1155/2021/4832864>

NIMH. (2019). NIMH Obsessive-Compulsive Disorder. [https://www.nimh.nih.gov/health/topics/obsessive-](https://www.nimh.nih.gov/health/topics/obsessive-compulsive-disorder-ocd)

[compulsive-disorder-ocd](https://www.nimh.nih.gov/health/topics/obsessive-compulsive-disorder-ocd)

Poldrack, R., Congdon, E., Triplett, W. *et al.* A genome-wide examination of neural and cognitive function. *Sci*

Data 3, 160110 (2016). <https://doi.org/10.1038/sdata.2016.110>

Terbeck, S., Akkus, F., Chesterman, L. P., & Hasler, G. (2015). The role of metabotropic glutamate receptor 5 in the

pathogenesis of mood disorders and addiction: combining preclinical evidence with human Positron

Emission Tomography (PET) studies. *Frontiers in neuroscience*, 9, 86.

<https://doi.org/10.3389/fnins.2015.00086>

Welch, J. M., Lu, J., Rodriguez, R. M., Trotta, N. C., Peca, J., Ding, J. D., Feliciano, C., Chen, M., Adams, J. P.,

Luo, J., Dudek, S. M., Weinberg, R. J., Calakos, N., Wetsel, W. C., & Feng, G. (2007). Cortico-striatal synaptic defects and OCD-like behaviours in Sapap3-mutant mice. *Nature*, 448(7156), 894–900.

<https://doi.org/10.1038/nature06104>

Wood, M. (2018, November 11). *Medication, therapy and now surgery offer hope for OCD*. Medication, therapy

and now surgery offer hope for OCD - UChicago Medicine. Retrieved November 28, 2022, from
<https://www.uchicagomedicine.org/forefront/neurosciences-articles/medication-therapy-and-now-surgery-offer-hope-for-severe-obsessive-compulsive-disorder#:~:text=At%20its%20most%20severe%2C%20however>

Woody, S. R., Steketee, G., & Chambless, D. L. (1995). Reliability and validity of the Yale-Brown Obsessive-

Compulsive Scale. *Behaviour Research and Therapy*, 33(5), 597–605. [https://doi.org/10.1016/0005-7967\(94\)00076-v](https://doi.org/10.1016/0005-7967(94)00076-v)

Xu, J., Hao, Q., Qian, R., Mu, X., Dai, M., Wu, Y., Tang, Y., Xie, M., & Wang, Q. (2021). Optimal Dose of Serotonin Reuptake Inhibitors for Obsessive-Compulsive Disorder in Adults: A Systematic Review and Dose–Response Meta-Analysis. *Frontiers in Psychiatry*, 12. <https://doi.org/10.3389/fpsyg.2021.717999>

Yi, D., Ahn, J., & Ji, S. (2020). An Effective Optimization Method for Machine Learning Based on ADAM. *Applied Sciences*, 10(3), Article 3. <https://doi.org/10.3390/app10031073>

Section VII: Code Availability

The code written and used in analysis for this project can be found at

<https://github.com/Tarune28/Modeling-T1-Resting-State-MRI-Variants-Using-Convolutional-Neural-Networks-in-Diagnosis-of-OCD>. Code used may be reused and modified from this project with appropriate attribution.

Section VIII: Appendices

Appendix A: Limitations and Assumptions

Limitations:

1. Utilization of more memory requiring models such as SVM were limited.
2. Training based on fractional anisotropy scan data rather than TRS-MRI in relation to the OCD model.
3. Computing power was limited to 8GB RAM.
4. Limitation to TRS-MRI scans due to motion distortion in fMRI scan data.

Assumptions:

1. Analysis using FSL conducted by Kim, Seung-Goo et al., 2015 was accurately conducted for Eddy correction.
2. Variations in heatmap outputs are solely due to the use of the global pooling layer.
3. Central 40 TRS-MRI scans pertain the most relevance to neural network models.

Appendix B: Example Engineering Matrix Title: The Comparison Between Reference Design A and Prototypes B-D

Criteria	Max Points	Design A	Design B	Design C	Design D
1. Efficiently Flushes the Toilet (required)	10	10	10	10	10
2. Overflow Option (required ≥ 7)	10	8	7	7	10
3. Back-up Water Supply	10	6	6	6	6
4. Aesthetically Pleasing	8	5	7	6	7
5. Easily Adaptable	7	6	7	7	6
6. Affordable	6	5	6	6	6
Total	51	40	43	42	45
Percent	100%	78%	84%	82%	88%

- Design A: (Exterior side tank method) Piping connects to the drain pipe of the sink and leads to a chamber just outside of the toilet tank, and when the toilet tank needs to be refilled for a flush it will release the water from the gray water collection chamber.
- Design B: (Interior tank method) Piping connects the drain pipes of the sink to a chamber resting inside the existing toilet tank, and uses the flapperless method of releasing water straight into the hole to flush the toilet.
- Design C: (Resting tank method) Piping connects the drain pipes of the sink to a chamber resting above the original toilet tank, and when flushed, water is released into a flapperless toilet chamber and flushes the toilet.
- Design D: (Drain collection method) Drain pipes of the sink empty into a chamber underneath the sink and then piping will carry the water to the toilet tank when it needs to be refilled.

